Posttranslational Modifications of the Lutropin Receptor: Mass Spectrometric Analysis†

Mai-Thu Vu-Hai,‡ Jean-Claude Huet,§ Klára Echasserieau,‡ Jean-Michel Bidart,|| Céline Floiras,§ Jean-Claude Pernollet,§ and Edwin Milgrom*,‡

Unité de Recherche INSERM Unité 135, Hormones, Gènes et Reproduction, Hôpital Bicêtre, 94275 Le Kremlin Bicêtre Cedex, France, Unité de Recherche INRA UR477, Biochimie et Structure des Protéines, 78352 Jouy-en-Josas Cedex, France, and Unité de Biochimie Clinique, Institut Gustave Roussy, 94805 Villejuif, France

Received December 21, 1999; Revised Manuscript Received March 1, 2000

ABSTRACT: Our present knowledge of the lutropin (LH/hCG) receptor structure derives from deductions made from its amino acid sequence as established by studying the cDNA. To obtain direct experimental information, luteinizing hormone (LH) receptor expressed in L cells was immunopurified in sufficient amounts to warrant analysis by mass spectrometry and microsequencing. The mature receptor, complexed to human chorionic gonadotropin (hCG), was purified by using monoclonal antibodies recognizing the hormone, whereas the mannose-rich non-hormone-binding precursor was purified by use of antireceptor antibodies. Determination of the N-terminus showed that $^2/_3$ of protein molecules started at Thr24 whereas $^1/_3$ started at Ala28. All these molecules bound hCG, suggesting that the most N-terminal region of the receptor does not participate in hormone binding. Six N-glycosylation sites have been predicted from the amino acid sequence. One of them (Asn299) was found to be nonglycosylated in both the precursor and the mature protein. The most heavily glycosylated residue was Asn291, followed by Asn195 and Asn99. These three sites accounted for 82% and 97% of carbohydrate moieties in the mature receptor and in the mannose-rich precursor, respectively. The presence of some receptor molecules nonglycosylated at sites 99, 174, and 195 in hormone−receptor complexes dismisses a direct role of these glycosylation sites in hormone binding or in the correct folding of the protein. The mature carbohydrate chains were homogeneous at position 174, 195, and 313 (absence of Golgi mannosidase II activity at positions 174 and 313, absence of GlcNAc tranferases III and IV activity at position 195). Heterologous carbohydrates were present at sites 99 and 291. The latter, which is highly variable in carbohydrate chains, is unlikely to participate in a direct interaction with hormone. Site 313 thus remains as the main candidate for a role in hormone binding.

Our present knowledge of the structure of the lutropin (LH)[1] receptor as well as that of other receptors of the same family (FSH and TSH receptors) derives from the sequencing of the corresponding cDNA (*1*−*4*). Comparison with various consensus sequences led to predictions of the site of cleavage of the signal peptide and thus of the N-terminus of the mature protein (*1*−*4*). A similar analysis also determined the probable existence of six N-glycosylation sites (*1*−*4*). Furthermore, hydrophobicity predictions led to the delineation of seven transmembrane spans, a large extracellular domain and a shorter intracellular domain. The extracellular domain was shown to be the site of hormone binding (*5*, *6*).

Our direct knowledge of the structure of the protein comes mainly from Western blot experiments, which allowed the detection of a large glycosylated protein of approximately 105 kDa as well as a precursor protein of ∼68 kDa. Deglycosylation either by endoglycosidase F, which excises all carbohydrates, or endoglycosidase H, which only clips out mannose-rich carbohydrate chains (present in the precursor), yielded a polypeptide backbone of ∼63 kDa (*7*). The receptor precursor present in the endoplasmic reticulum (*8*, *9*) is deficient in hormone binding (*7*) and its exact physiological role is presently unknown. The presence in relatively high concentration of a mannose-rich precursor has also been described for the other gonadotropin receptor (FSH receptor) in target organs (*10*).

In the present study, we used L cells permanently transformed with an expression vector encoding the LH receptor and immunopurification procedures to isolate in relatively high amounts both the receptor and the precursor. Monoclonal antibodies against the hormone (*11*) allowed us to isolate hormone−receptor complexes that corresponded only to the mature receptor. The flowthrough of this immunopurification column contained the precursor, which is deficient in hormone binding. It was applied to an

† This work was supported by INSERM, the Faculté de Medecine Paris Sud, the Assistance Publique-Hôpitaux de Paris, the INRA, and the Association pour la Recherche sur le Cancer.

* Corresponding author: Phone 33-1 45 21 33 29; Fax 33-1 45 21 27 51; E-mail u135@kb.inserm.fr.

‡ Hôpital Bicêtre.

§ Biochimie et Structure des Protéines.

|| Institut Gustave Roussy.

[1] Abbreviations: LH, luteinizing hormone; hCG, human chorionic gonadotropin; TSH, thyroid-stimulating hormone; FSH, follicle-stimulating hormone; MALDI, matrix-assisted laser desorption ionization; TOF, time-of-flight.

10.1021/bi992913f CCC: $19.00
Published on Web 04/13/2000

immunomatrix containing anti-LH receptor monoclonal antibodies, allowing the isolation of the precursor.

MATERIALS AND METHODS

Chemicals. Methanol and acetonitrile were provided by Perkin-Elmer Biosystems, water (HPLC-grade), EDTA, and calcium chloride by Merck, guanidine hydrochloride, formic acid, 5 M ammonium acetate, iodoacetamide, and ammonium hydrogenocarbonate by Fluka, dithiothreitol by Serva, 95% ethanol and trichloroacetic acid by Prolabo, β-mercaptoethanol and Tris-HCl by Sigma, Zwittergent 3−16 by Calbiochem, hCG by Organon, and acrylamide and Affi-Gel 10 by Bio-Rad. All other chemicals were of the highest purity commercially available.

Receptor Expression and Purification. L cells permanently transformed with an expression vector encoding the porcine LH receptor were used (*7*). In most cases the cells were incubated with 50 nM hCG for 2 h at 4 °C. The cells (∼15 g) were scraped and washed twice. The cellular pellet was homogenized with a Dounce apparatus in 200 mL of 25 mM Hepes buffer, pH 7.4. The pellet obtained after a 40 000 rpm centrifugation for 30 min at 4 °C in a Ti45 rotor (Spinco) was extracted with 200 mL of the same buffer containing 1.2% Triton X-100. The supernatant was clarified by a centrifugation at 105000*g* for 65 min at 4 °C and chromatographed through a column (1.5 mL) of Affi-Gel 10 coupled to D_1E_8 antibody (8 mg of antibody/mL of gel). D_1E_8 antibody, which binds hCG even when the latter is complexed with the receptor, has been previously described (*11*, *12*). The column was extensively washed (*7*, *12*) and hCG−receptor complexes were eluted in 3 mL of 10 mM ammonium bicarbonate buffer, pH 10.5. This yielded ∼200 pmol of mature receptor.

The flowthrough of the column, which contained ligand-free LH receptor, was applied to a column (1.5 mL) of Affi-Gel 10 coupled to anti-receptor antibody LHR38 (*7*, *12*) (8 mg/mL). After extensive washing, the receptor precursor (∼200 pmol) was eluted in 1% formic acid (3 mL).

In some cases the cells were not incubated with hormone and the Triton X-100 membrane extract was directly applied to the LHR38-Affi-Gel 10 column. This yielded ∼400 pmol of a mixture of mature and precursor receptors. The latter were separated by electrophoresis in denaturing conditions as previously described (*12*). The proteins were electroblotted on poly(vinylidene difluoride) (PVDF) membranes (*13*). The bands corresponding to the mature receptor and to the precursor were excised and used for further analysis.

Protein Adsorption on PVDF Membranes. Prospin (Applied Biosystems) cartridges deprived of the 3 kDa cutoff filter were wetted with methanol and washed with water. Proteins were adsorbed by 400 μL aliquots and centrifuged for 5 min at 1500*g* at 20 °C in a Hettich universal 16R centrifuge with a 1612 rotor (*14*). PVDF membranes were washed twice with water (200 μL) before being dried. They were cut off with a punch prior to further treatment.

Reduction and Alkylation. PVDF membranes were cut into small pieces and wetted with 5 μL of methanol. The proteins were reduced with 10 mM dithiothreitol in 200 μL of 67 mM Tris-HCl, 0.7 mM EDTA, pH 8.2, and 6 M guanidine hydrochloride for 1 h at 50 °C and then alkylated with 20 mM iodoacetamide for 1 h at room temperature in the dark. Alkylation was halted by addition of β mercaptoethanol (2% v/v). Membranes were washed 5 times with water (400 μL) to eliminate salts and reagents.

Tryptic Digestion. The digestion was performed on reduced and alkylated receptors on PVDF membranes in a mixture of 0.2 M ammonium hydrogenocarbonate, pH 8.0, and 1% (w/v) Zwittergent 3−16 (*15*) with 0.5 μg of modified trypsin (Promega sequencing grade) in 20 μL at 37 °C during 18−20 h and the reaction was stopped with formic acid.

High-Performance Liquid Chromatography Coupled with Ion-Spray Mass Spectrometry and Edman Sequencing. Peptides were separated by reverse-phase high-performance liquid chromatography (RPLC) on-line coupled with an ion-spray mass spectrometer (IS-MS) (Perkin-Elmer Sciex API100). RPLC was run with a Perkin-Elmer device (Applied Biosystems pump 140D and UV detector 785 with U-shaped fused silica tubing, 7 mm path length) on a C18 RP 300 capillary LC column (0.5 × 150 mm, 300 Å) at controlled temperature (40 °C). The gradient was made by mixing solvent A [0.1% (v/v) Fluka formic acid and 4 mM Fluka ammonium acetate in Merck HPLC water] with solvent B [90% Perkin-Elmer acetonitrile, 0.1% (v/v) Fluka formic acid, and 4 mM Fluka ammonium acetate in Merck HPLC water] at a flow rate of 5 μL/min. The acetonitrile gradient began at 4.5%, increased linearly to 9% in 15 min, then to 51% in 100 min, then to 85.5% in 10 min, remained constant for 20 min, was lowered down to 45% in 10 min, and ended with a continuous wash at this concentration.

After being monitored for absorbance at 215 nm, the flow was split between the micro-ion-spray source (0.3 μL/min) and a fraction collector device (Perkin-Elmer Biosystems Microblotter 173 A) which led to peptides blotted onto Problot PVDF membrane. IS-MS experiments were controlled with the Sample Control 1.3 software using a positive mode from 400 to 2100 amu with 0.2 amu steps and a 0.4 ms dwell-time. The ion spray needle voltage was + 5000 V and the orifice plate voltage + 40 V. The spectrometer was standardized with a mixture of poly(propylene glycol) (PPG) 425, 1000, and 2000. Mass spectrometry data were analyzed with the Perkin-Elmer Sciex Bio-Multi-View 1.2 software. The average molar masses were calculated from the sequence with the Perkin-Elmer Sciex Peptide Map 2.2 software. Peptide fractions from the PVDF membrane were cut out with a scalpel and treated with 0.1 mg of biobrene (*16*) prior to loading into the sequencer.

N-Terminal Sequencing. Automated Edman sequencing was performed on a Perkin-Elmer Applied Biosystems Procise 494A sequencer with reagents and methods from the manufacturer (Applied Biosystems).

RESULTS

To identify the sites and nature of the posttranslational modifications, we submitted both the mannose-rich precursor and the mature receptor to trypsinolysis. Amino acids are numbered from the N-terminal Met of the leader sequence.

Purification of the Mature LH Receptor and of the Mannose-Rich Precursor. Immunopurification of hCG−receptor complexes with anti-hCG antibodies yielded the mature form of the receptor (Figure 1, lane b). Edman sequencing of this preparation showed that 45% of N-termini corresponded to the receptor, 45% to hCG, and 10% to contaminants.

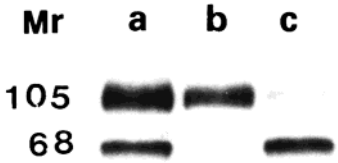

FIGURE 1: Western blot showing the purification of the mature LH receptor and of the mannose-rich precursor. Lane a: Triton X-100 membrane extracts were immunopurified on an immunomatrix containing antireceptor antibodies. Lanes b and c: Cells were incubated with hCG. Membrane extracts were passed on an immunomatrix containing anti hCG antibodies. The eluate of this column is shown in lane b. The flowthrough of the column was applied to an immunomatrix containing anti-LH receptor antibodies. The eluate of the latter column is shown in lane c. An aliquot (3 μL) of each eluate was analyzed by immunoblot using an antireceptor antibody LHR 775 (*7*, *12*). The mature receptor had an apparent molecular mass of 105 kDa, and the precursor, 68 kDa.

The flowthrough of the gel carrying anti-hCG antibodies was applied to an immunomatrix carrying antireceptor antibodies. This yielded mainly the mannose-rich precursor with a minor proportion of mature receptor (Figure 1, lane c). The latter was either free of hormone or had not previously bound to the anti-hCG immunomatrix. In this preparation, Edman sequencing showed 80% of N-termini corresponding to the receptor and 20% to various contaminants including some hCG.

Figure 1, lane a shows a mixture of mature receptor and of mannose-rich precursor as obtained in an experiment where the membrane extract was directly submitted to immunochromatography on a gel containing antireceptor antibodies.

Signal Peptide Cleavage Sites. The N-terminal sequencing of both the mannose-rich precursor and of the mature undigested receptor as well as the sequence of the HPLC-isolated N-terminal peptides led to the simultaneous observation of two N-terminal ends. Thr24 and Ala28, accounting for $^2/_3$ and $^1/_3$ of the molecules, respectively. The same proportions were observed in the mature receptor and in the precursor.

Location of the Glycosylation Sites in the Mannose-Rich Precursor. The HPLC chromatogram of the mannose-rich receptor tryptic peptides is presented in Figure 2. The whole chromatogram was thoroughly analyzed by both mass spectrometry and sequencing. All the putative cleaved peptides of the ectodomain were observed and identified by both mass spectrometry and sequencing, with the exception of the peptide 220−222, too short to be separated. To focus the results on the posttranslational modification sites, only those peptides bearing the putative N-glycosylation sites are shown in Figure 2.

The mass spectrum of peptide I89−K109, which originates from the mannose-rich precursor, is shown in Figure S1 (Supporting Information). This peptide includes the N99 site of glycosylation.

During the mass spectrum acquisition of a given chromatographic peak corresponding to a glycosylated peptide, the carbohydrate chains were progressively deglycosylated. This gave rise to complex spectra composed of families of 4−6 molecules differing in mass one from the other by one hexose (mannose) residue (162 amu). This observation ascertained the nature of the posttranslational modification. We only report in Table 1 the molar masses of the largest forms. For each peptide the comparison of the calculated mass with the measured mass led to a difference that could be unambiguously attributed to high-mannose-type carbohydrates (two *N*-acetylglucosamines and several mannoses) as reported in Table 1. With the exception of site 299, all the putative sites were found to be glycosylated. Using the total ion counts observed by mass spectrometry, which may

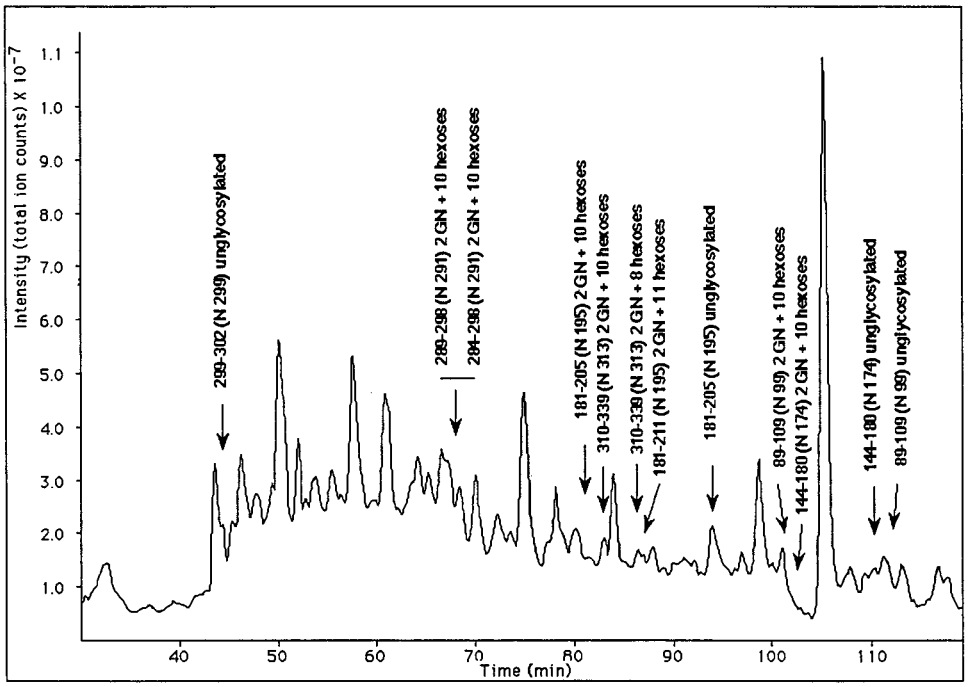

FIGURE 2: Chromatogram of the tryptic digest of the mannose-rich receptor precursor. Only the peptides bearing a putative glycosylation site are indicated by arrows. Their positions and lengths, identified by Edman sequencing and mass spectrometry, are first indicated. The N-glycosylation site is noted in parentheses, followed by the number of hexose residues occurring after the two first *N*-acetyl glucosamines (GN).

Table 1: Characterization of the Ectodomain Peptides Bearing an N-glycosylation Site in the Mannose-Rich Receptor Precursor

site	retention time (min)	peptide position	polypeptide calculated mass[a] (amu)	measured mass (amu)	difference	proposed carbohydrate chain	calculated carbohydrate	abundance ion counts (cpm × 10^{-6})
N 99	101.3	89−109	2373.7	4401	2027.3	2GN-10 hexoses	2027.8	20
	113.2	89−109	2373.7	2373.1	−0.6	unglycosylated	0	8
						total		28
N 174	103.2	144−180	4229.8	6260	2030.2	2GN-10 hexoses	2027.8	1.4
	110.6	144−180	4229.8	4229.9	0.1	unglycosylated	0	2.5
						total		3.9
N 195	80.9	181−205	2782.1	4809	2026.9	2GN-10 hexoses	2027.8	20
	87.1	181−211	3474.9	5670	2195.1	2GN-11 hexoses	2190.0	1.5
	94.1	181−205	2782.1	2780	−2.1	unglycosylated	0	9
						total		30.5
N 291	68.6	289−298	1246.4	3274	2027.6	2GN-10 hexoses	2027.8	43
	74	284−298	1800.1	3828	2028.0	2GN-10 hexoses	2027.8	20
						total		63
N 299	44.2−44.5	299−302	494.5	494.2	−0.3	unglycosylated	0	2.1
						total		2.1
N 313	83.4	310−339	3575.8	5603	2027.2	2GN-10 hexoses	2027.8	1.3
	86.2−86.9	310−339	3575.8	5281	1705.2	2GN− 8 hexoses	1703.5	0.15
						total		1.45
						total		128.95

[a] Masses are calculated with the average natural isotopic abundance.

Table 2: Relative Abundance of Carbohydrates at the Glycosylation Sites in the Mannose-Rich Precursor and the Mature Receptor[a]

	sites						
	99	174	195	291	299	313	total
			Mannose-Rich Precursor				
unglycosylated forms (cpm × 10^{-6})	8	2.5	9	0	2.1	0	21.6
glycosylated forms (cpm × 10^{-6})	20	1.4	21.5	63	0	1.45	107.35
proportion of glycosylated site (%)	71.4	35.9	70.5	100.0	0.0	100.0	
proportion of glycosylation (%)	18.6	1.3	20.0	58.7	0.0	1.4	100.0
			Mature LH Receptor				
unglycosylated forms (cpm × 10^{-6})	3	0.9	1.1	0	0.9	0	5.9
glycosylated forms (cpm × 10^{-6})	15.6	4.4	21.2	28.8	0	10.2	80.2
proportion of glycosylated site (%)	83.9	83.0	95.1	100.0	0.0	100.0	
proportion of glycosylation (%)	19.5	5.5	26.4	35.9	0.0	12.7	100.0
observation	heterogeneous	homogeneous	homogeneous	heterogeneous	−	homogeneous	

[a] Abundance is measured as the total ion counts expressed in counts per minute.

roughly represent the abundance of the glycosylated peptides, we inferred the relative amount of carbohydrates at each site. The level of glycosylation varied largely at the different sites. As reported in Table 2, position 99 accounted for 18.6% of the glycosylated peptides, position 174 for 1.3%, position 195 for 20.0%, position 291 for 58.7%, position 299 for 0%, and position 313 for 1.4%. Three sites (99, 195, and 291) accounted for 97.3% of the carbohydrate moieties.

Nature of the Carbohydrates at Each Glycosylated Site of the Mature Receptor. A similar analysis was performed with the mature receptor. The HPLC chromatograms are reported in Figure S2 (Supporting Information). Due to the variable glycosylation caused by incomplete and/or multiple processing, the number of glycosylated peptides largely increased in number, while the abundance of each peptide was significantly decreased. Only peptides identified by both mass spectrometry and N-terminal sequencing were considered to be relevant and reported in Table 3. Due to the number of peptides, only regions where peptides bearing the glycosylation sites were found are reported in Figure S2A. The precise position of the peptides analyzed is reported in detail in Figure S2B−F.

At each glycosylated site, several carbohydrate chains were simultaneously observed. Some of them were partly deglycosylated high-mannose chains, but most consisted of processed carbohydrate chains. Complete antennae were often accompanied by precursors. Those observed are summarized in Table 3. The comparison for each peptide of the calculated mass with the measured mass led to a difference that could be attributed to complex precursor and complete carbohydrate structures numbered according to Figure 3.

Using the total ion counts, we inferred the approximate relative amount of carbohydrates at each site. As reported in Table 2, the unglycosylated peptides were much less abundant than in the mannose-rich receptor. As in the mannose-rich receptor, the level of glycosylation largely varied from one site to the other. Position 99 accounted for 19.5% of the glycosylated peptides, position 174 for 5.5%, position 195 for 26.4%, position 291 for 35.9%, and position 313 for 12.7%. No carbohydrate moiety was observed linked to N299. The three sites 99, 195, and 291 accounted for 81.8% of the carbohydrate moieties, whereas the same sites

Table 3: Characterization of the Ectodomain Peptides Bearing a N-glycosylation Site in the Mature Receptor[a]

site	retention time (min)	peptide position	polypeptide calculated mass (amu)	measured mass (amu)	difference	proposed carbohydrate chain	calculated carbohydrate	abundance ion counts (cpm × 10^{-6})
N 99	109.1	89−109	2373.7	2373.6	−0.1	unglycosylated	0	3
	99	89−124	4059.6	4468	408.3	2GN	406.4	1
	94.5	89−109	2373.7	3100	726.3	2GN-2 hexoses	730.7	0.9
	−	89−109	2373.7	3266	892.3	2GN-3 hexoses	892.8	2.4
	93.1	89−124	4059.6	5599	1539.4	2GN-7 hexoses	1541.4	1.5
	95.3	89−126	4301.0	5840	1539.0	2GN-7 hexoses	1541.4	0.7
	95.2	89−109	2373.7	3467	1093.3	structure VIII	1096.0	1.9
	93.1	89−126	4301.0	5599	1298.0	structure IX	1299.2	1.5
	91.7	89−124	4059.7	5562	1502.4	structure X	1502.4	1.2
	95.2	89−109	2373.7	3591	1217.3	structure VI	1217.1	0.3
	95.2	89−109	2373.7	3875	1501.3	structure X	1502.4	0.7
	99.1	89−126	4301.0	6363	2062.0	structure XII	2060.9	0.9
	101.3	89−109	2373.7	6103	3729.3	structure XIV	3729.3	0.4
	92.6	89−109	2373.7	4452	2078.3	structure XVIII	2076.9	1.4
	99	89−109	2373.7	4468	2094.3	structure XVIII	2092.9	0.8
						total		18.6
N 174	96.3	144−180	4229.8	4228	−1.8	unglycosylated	0	0.9
	78.9	144−180	4229.8	5126	896.2	2GN+3 hexoses	892.8	0.6
	101.3	138−180	4886.6	6103	1216.4	structure VI	1217.1	0.4
	78.5	138−180	4886.6	6301	1414.4	structure VII	1420.3	2.8
	78.3	144−180	4229.8	6756	2526.2	structure XVII	2530.3	0.6
						total		5.3
N 195	73.5	181−211	3474.9	3474	−0.9	unglycosylated	0	1.1
	73.3	181−205	2782.1	2983	200.9	1GN	203.2	1.3
	75.0	181−205	2782.1	3185	402.9	2GN	406.4	6.5
	79.0	181−211	3474.9	3884	409.1	2GN	406.4	1.4
	76.0	181−205	2782.1	4822	2039.9	2GN-10 hexoses	2027.8	1.3
	75.0	181−211	3474.9	4574	1099.1	structure VIII	1096.0	8.5
	75.8	181−205	2782.1	5138	2355.9	structure XII	2352.2	2.2
						total		22.3
N 291	66.7	289−298	1246.4	2788	1541.6	2GN-7 hexoses	1541.4	1.3
	54.5	289−298	1246.4	2141	894.6	2GN-3 hexoses	892.8	4.2
	58.2	289−298	1246.4	2662	1415.6	structure VII	1420.3	2.9
	64.5	289−298	1246.4	2342	1095.6	structure VIII	1096.0	1.3
	67.4	284−309	3109.5	4412	1302.5	structure IX	1299.2	3.6
	55.1	289−309	2555.8	4058	1502.2	structure X	1502.4	1.8
	67.3	289−309	2555.8	4057	1501.1	structure X	1502.4	1.8
	67.9	289−298	1246.4	2747	1500.6	structure X	1502.4	1.8
	79.2	289−310	2714.9	4213	1498.1	structure X	1502.4	1.1
	54.9	284−298	1800.1	3506	1706.0	structure XI	1705.6	1.8
	74.7	289−302	1722.9	4075	2352.1	structure XII	2352.2	1.6
	66.8	284−298	1800.1	4184	2384.0	structure XII	2384.2	3.8
	63.7	289−302	1722.9	3346	1623.1	structure XV or XVI	1623.5	1.8
						total		28.8
N 299	39.4	299−302	494.6	493.4	−1.2	unglycosylated	0	0.9
						total		0.9
N 313	75.9	310−339	3575.8	3988	412.2	2GN	406.4	1.8
	98.0	310−339	3575.8	4469	893.2	2GN-3 hexoses	892.8	2.8
	100	310−339	3575.8	4468	892.2	2GN-3 hexoses	892.8	0.8
	72.7	310−339	3575.8	5113	1537.2	2GN-7 hexoses	1541.4	0.6
	81.8	310−339	3575.8	4994	1418.2	structure VII	1420.3	3.8
	101.3	310−339	3575.8	6103	2527.2	structure XVII	2530.3	0.4
						total		10.2
						total		85.2

[a] Measures are calculated with the average natural isotopic abundance. Complex precursor and complete carbohydrate structures are numbered according to Figure 4. All possible variants of structures XII, XIII, XIV, XVII, and XVIII indicated in Figure 4 are named after a common term respective to each structure type.

accounted for 97.3% of carbohydrates in the mannose-rich precursor.

A close examination of the peptide map allows us to observe the nature of the carbohydrates found at each site (Table 3). At position 99, beside several peptides (accounting for 35% of the glycosylated peptides) that bear partly deglycosylated high-mannose chains, several transient complex structures (structures VI, VIII, IX and X) were observed. They corresponded to three processing pathways leading to the complete structures XVIII (bisected biantennary hybrid), XII (biantennary complex), and XIV (tetraantennary complex) as shown in Figure 3. These transient structures accounted for 30.1% of the glycosylated peptides and the complete structures for 18.8%. A peptide containing unglycosylated N99 was observed, confirming the observation in the mannose-rich precursor and accounting for 16.1% of the N99 peptides.

At position 174, 17% of the peptides were totally unglycosylated and 11.3% had partly deglycosylated high-mannose chains. Two transient structures (VI and VII) (accounting for 60.4% of the carbohydrates) were observed together with the sole complete structure XVII (triantennary hybrid) (11.3%

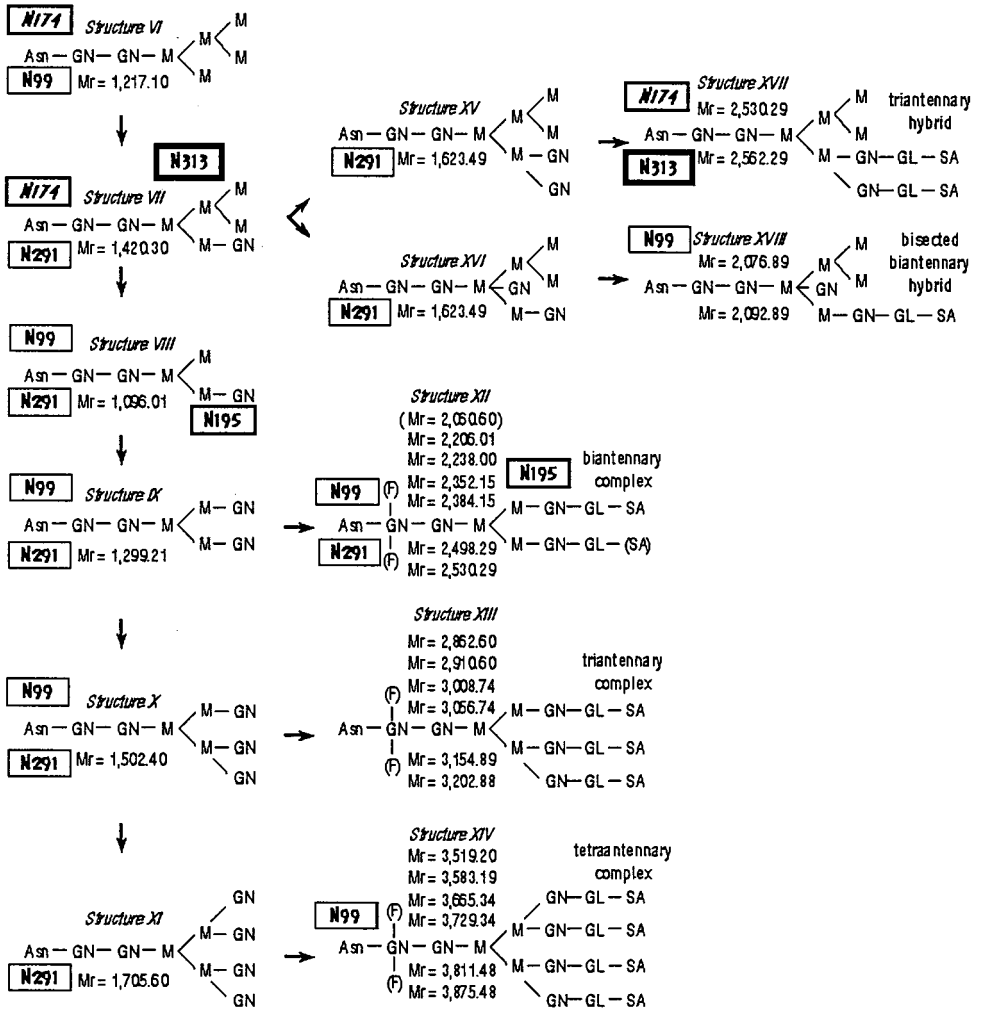

FIGURE 3: Carbohydrate chain biosynthesis pathways involved in the glycosylation of the mature receptor. The molecular weights are indicated by M_r. Abbreviations: Asn, asparagine; M, mannose; GN, *N*-acetylglucosamine; GL, galactose; F, fucose; SA, sialic acid (or alternatively *N*-glycolylneuraminic acid). Positions where the carbohydrates were found are indicated by numbers in boxes. Bold frames indicate those where carbohydrate moieties originated from a single metabolic pathway.

of the carbohydrates). Only one glycosylation pathway was observed, showing the absence of the Golgi mannosidase II activity at this site. At position 195, 4.9% of the peptides were totally unglycosylated and 47.1% bear partly deglycosylated high-mannose chains. The precursor structure VIII was observed (38.1%) together with the only complete structure XII (biantennary complex) accounting for 9.9% of the carbohydrates. In this case, only one pathway was observed, dismissing the occurrence of any activity of GlcNAc transferases III and IV at this site. Figure S3 (Supporting Information) shows the mass spectra of peptides originating from the mature receptor and encompassing the glycosylated N99 and N195 sites. Concerning site 291, no unglycosylated peptide was observed, but 19.1% of the peptides had partly deglycosylated high-mannose chains. The complete structure XII (biantennary complex) accounting for 18.8% of the carbohydrates was observed with its precursor forms VII, VIII, and IX (27.1%). Neither the complete forms (hybrid structures XVII and XVIII) corresponding to the terminal processing of structures XV and XVI (accounting for 6.2%) nor those corresponding to the processing of the transient structures X and XI (accounting for 28.8%) leading to the complete structure XIII and/or XIV (tetraantennary complex) were observed. It is likely that the enzymatic processing was only partial at this site. At least three pathways were consequently observed to occur at position 291.

The unglycosylated 299 site of the precursor receptor was found again to be unglycosylated in the mature form. The absence of glycosylation at this position was observed not only in peptides beginning at position 299 but also in peptides beginning at position 289 and ending after 299 in which only the site N291 was observed to be glycosylated.

Only the complete structure XVII (triantennary hybrid) was observed at site 313, representing 3.9% of the total ion counts, whereas the amount of the precursor form VII was 37.3%. At this position, the partly deglycosylated high-mannose chains accounted for 58.8%. Thus only one pathway was observed, dismissing the occurrence of the Golgi α-mannosidase II at this site.

DISCUSSION

The direct study of membrane receptor structure and especially that of G-protein-coupled receptors has been hampered by the difficulty of purifying them in sufficiently large amounts. Bacteriorhodopsin and rhodopsin are exceptions in this respect due to their high cellular concentrations

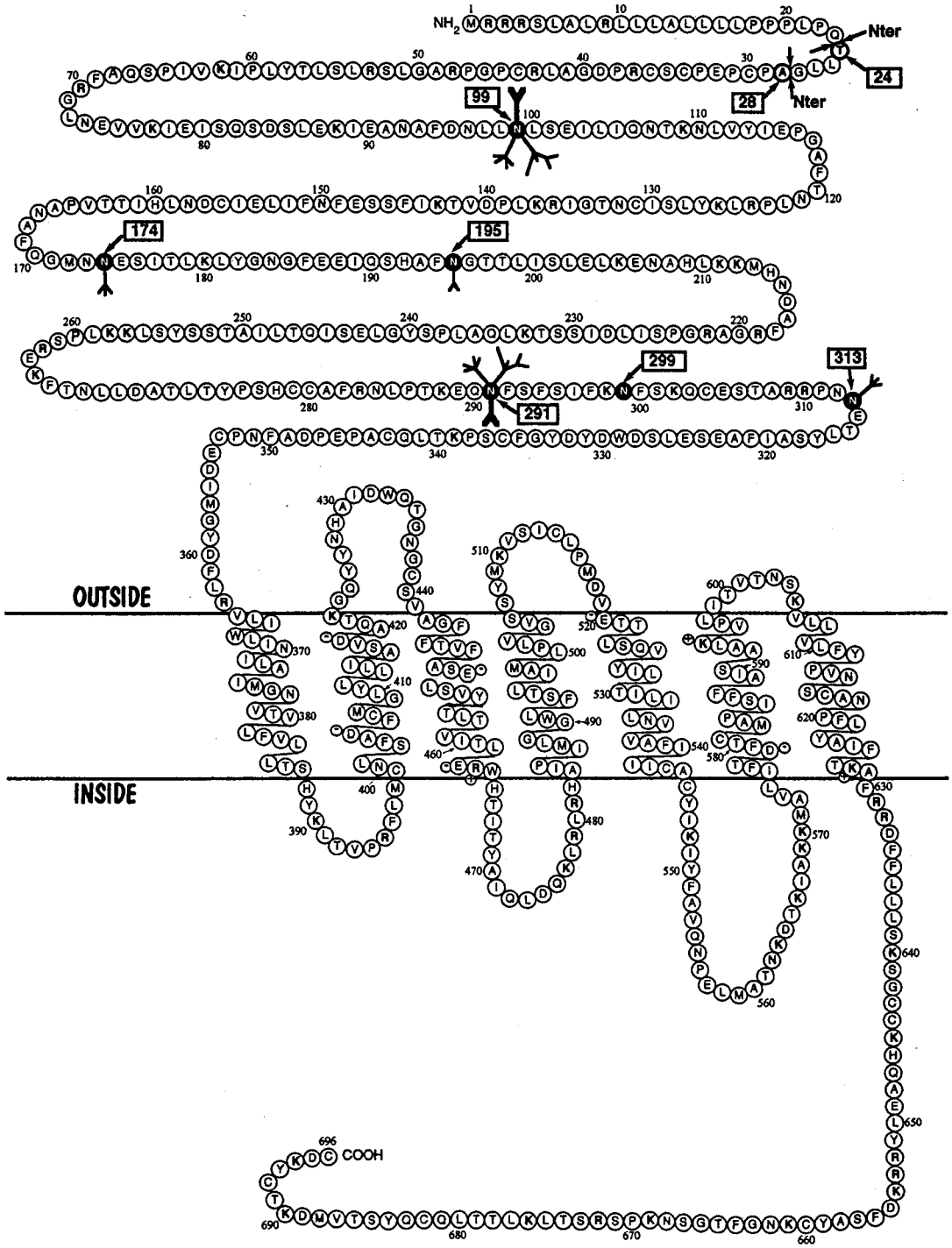

FIGURE 4: Location of basal posttranslational modifications in the mature LH receptor. Nter indicates the N-terminus of the processed protein; the potential N-glycosylation sites are indicated by a black circle with N; the observed carbohydrate antennae are summarized at each site.

(*17*). Very recently a mass spectrometric study of bradykinin B_2 receptor palmitoylation and phosphorylation has been reported (*18*). MALDI-TOF mass spectrometry has also been used in addition to other methods to study phosphorylation of the β_2 adrenergic receptor (*19*).

The structure of the ectodomain of gonadotropin and thyrotropin receptors has been the subject of great interest since it is the region where the hormone is bound (*5*, *6*). Protein modeling (*20, 21*) and in vitro mutagenesis (*22*−*24*) are currently being used to try to understand receptor−hormone interactions. The possibility of devising new agonists or antagonists has been one of the reasons for the undertaking of such studies.

The mannose-rich precursors of most glycoproteins are present only in trace amounts. For an unknown reason, this is not the case for gonadotropin receptors. Mannose-rich precursors of the latter are present in large concentrations in the target cells (*7, 10*). We have been able to purify sufficient amounts of LH receptor and its precursor by immunochromatography to study some of their posttranslational modifications (Figure 4).

N-Terminal Ends of the Receptor. Receptor structures derived from cDNA sequencing predicted a single N-terminus in all cases (*1*−*4*). We show here that there is heterogeneity in receptor molecules and that two cleavage sites are being used for signal peptide excision. It is noteworthy that the purification procedure used to isolate the mature receptor (affinity with the hormone) ensured that the studied molecules were indeed able to bind the hormone. Since the dual N-terminal ends were found to occur in both the hormone-binding and nonbinding fractions of the receptor, it is likely that the extreme N-terminus is not involved in interactions with the ligand. It should be noted that a region immediately downstream of the N-terminus has been suggested to be crucial for hormone binding (*23*).

Glycosylation of the Receptor. Six different glycosylation sites have been predicted from the amino acid sequence of the pig LH receptor (*1*). These sites are completely conserved in the rat (*2*) and human (*3, 4*) receptors and thus the same sites of glycosylation were predicted in these species. The glycosylation of rat receptor was also studied by other indirect methods: in vitro mutagenesis of the predicted glycosylation sites followed by endoglycosidase digestion and comparison with the results of cell incubation with tunicamycin. Conflicting results were reported: one group (*25*) concluded that all six sites were indeed glycosylated, another group (*26*) that the site at position 99 (77 in their numbering) was not glycosylated.

The functional role of LH receptor glycosylation has also been a subject of controversy. Some groups have reported that carbohydrates are not required for hormone binding (*25, 27*−*31*), whereas others have suggested a role of the carbohydrates in hormone binding and/or correct folding of the protein (*26, 32*).

Petäjä-Repo (*33*) used glycosidase treatment and probing with labeled lectins to analyze carbohydrates in the rat LH receptor. The conclusion of these studies was that the receptor contains at least two complex oligosaccharide chains, of which one is biantennary and the rest are multiantennary. Our present study establishes the existence of five mature oligosaccharide chains, of which three are monoantennary and two are multiantennary.

Comparison of the Glycosylation of the Mannose-Rich Precursor and of the Mature Receptor. In both forms, only five among the six putative N-glycosylation sites are indeed subject to glycosylation, excluding any glycosylation at the N299 site. The comparison of the glycosylated sites of the mannose-rich receptor with the mature form clearly shows that the absence of glycosylation at position 299 is not due to a lack of processing duration. When the mannose-rich and the mature receptor are compared, the relative amounts of glycosylation at each site are in very good agreement. The two sites (99 and 174) that are largely the most glycosylated in the mannose-rich protein are also the most glycosylated in the mature receptor. The only exception is an increased glycosylation in the mature form in the least glycosylated sites (see for instance site 313) of the mannose-rich precursor (see Table 2). In general the mature receptor appears to be more glycosylated than the mannose-rich form. A contaminating calnexin sequence was observed associated with the mannose-rich receptor (results not shown). This strongly suggests that some of the mannose-rich molecules were still in the process of biosynthesis when analyzed.

Glycosylation Types in the Mature Receptor. For each glycosylated site, several carbohydrate chains were simultaneously observed. Some of them were partly deglycosylated high-mannose chains, but many consisted of processed carbohydrate chains, including precursors and complete antennae (Figure 3). The presence of a series of peptide masses in agreement with the metabolic pathways of carbohydrate chains allowed us to deduce the nature of the chains.

The processed glycosylation forms observed at each site corresponded to different pathways that occurred simultaneously (N99 and N291), leading to the formation of different carbohydrate forms (bisected biantennary hybrid, biantennal complex, and tetraantennary complex). Only a biantennary complex was found to occur at position 195, and a triantennary hybrid at both sites 174 and 313. There was a correlation between the level and the complexity of glycosylation, since the two heterogeneous sites accounted for more than 70% of the carbohydrate moieties.

The completion of the glycosylation at each site varied from one site to the other. The diversity of the mature carbohydrate chains probably reflected the difference in speed at which the oligosaccharides were combined. It is also worth noticing that the sites with antennae originating from the shortest metabolic pathways were found to comprise much more complete chains than those involving a greater number of biosynthetic steps.

Some receptor molecules were found nonglycosylated at sites 99, 174, and 195. These molecules were isolated as hormone-receptor complexes, which shows that glycosylation at these sites is not necessary for hormone binding nor for the proper folding of the protein. Among the remaining sites, site 291, which is much more heterogeneous in its carbohydrate chains than site 313, is thus unlikely to participate in a direct interaction with the hormone. The main possible candidate for a role in hormone binding thus remains glycosylation at site 313.

CONCLUSION

Mass spectrometric analyses and microsequencing of the LH receptor and of its precursor reveal the heterogeneity of this protein in terms of its N-terminus as well as N-glycosylation. They also show that structural predictions derived from amino acid sequences are not always verified. In vitro mutagenesis experiments also led to some unsubstantiated conclusions. In all cases these indirect approaches must be confirmed by the direct experimental study of the protein.

ACKNOWLEDGMENT

The manuscript was typed by A. D. Dakhlia.

SUPPORTING INFORMATION AVAILABLE

Three figures, showing the mass spectrum of peptide I89−K109 originating from the mannose-rich precursor, chromatogram of the tryptic digest of the mature receptor, and mass spectra of peptides originating from the mature receptor and encompassing glycosylated N99 and N195 sites. This material is available free of charge via the Internet at http://pubs.acs.org.

REFERENCES

1. Loosfelt, H., Misrahi, M., Atger, M., Salesse, R., Vu Hai, M. T., Jolivet, A., Guiochon-Mantel, A., Sar, S., Jallal, B., Garnier, J., and Milgrom, E. (1989) Cloning and sequencing of porcine LH−hCG receptor cDNA: variants lacking transmembrane domain, *Science 245*, 525−528.
2. McFarland, K. C., Sprengel, R., Phillips, H. S., Köhler, M., Rosemblit, N., Nickolics, K., Segaloff, D. L., and Seeburg, P. H. (1989) Lutropin−choriogonadotropin receptor: an unusual member of the G protein-coupled receptor family, *Science 245*, 494−499.
3. Minegishi, T., Nakamura, K., Takakura, Y., Miyamoto, K., Hasegawa, Y., Ibuki, Y., and Igarashi, M. (1990) Cloning and sequencing of human LH/hCG receptor DNA, *Biochem. Biophys. Res. Commun. 172*, 1049−1054.
4. Atger, M., Misrahi, M., Sar, S., Le Flem, L., Dessen, P., and Milgrom, E. (1995) Structure of the human luteinizing hormone−choriogonadotropin receptor gene: unusual promoter and 5′ noncoding region, *Mol. Cell. Endocrinol. 111*, 113−123.
5. Xie, Y. B., Wang, H., and Segaloff, D. L. (1990) Extracellular domain of lutropin/choriogonadotropin receptor expressed in transfected cells binds choriogonadotropin with high affinity, *J. Biol. Chem. 265*, 21411−21414.
6. Tsai-Morris, C. H., Buczko, E., Wang, W., and Dufau, M. L. (1990) Intronic nature of the rat luteinizing hormone receptor gene defines a soluble receptor subspecies with hormone binding activity, *J. Biol. Chem. 265*, 19385−19388.
7. Vu Hai, M. T., Misrahi, M., Houllier, M., Jolivet, A., and Milgrom, E. (1992) Variant forms of the pig lutropin/choriogonadotropin receptor, *Biochemistry 31*, 8377−8383.
8. Misrahi, M., Ghinea, N., Sar, S., Saunier, B., Jolivet, A., Loosfelt, H., Cerutti, M., Devauchelle, G., and Milgrom, E. (1994) Processing of the precursors of the human TSH receptor in various eukaryotic cells (human thyrocytes, transfected L cells and baculovirus infected insect cells), *Eur. J. Biochem. 222*, 711−719.
9. Hipkin, R. W., Sanchez-Yague, J., and Ascoli, M. (1992) Identification and characterization of a luteinizing hormone/chorionic gonadotropin (LH/CG) receptor precursor in a human kidney cell line stably transfected with the rat luteal LH/CG receptor complementary DNA, *Mol. Endocrinol. 6*, 2210−2218.
10. Vannier, B., Loosfelt, H., Meduri, G., Pichon, C., and Milgrom, E. (1996) Anti-human FSH receptor monoclonal antibodies: immunochemical and immunocytochemical characterization of the receptor, *Biochemistry 35*, 1359−1366.
11. Bidart, J. M., Troalen, F., Bohuon, C. J., Hennen, G., and Bellet, D. H. (1987) Immunochemical mapping of a specific domain on human choriogonadotropin using anti-protein and anti-peptide monoclonal antibodies, *J. Biol. Chem. 262*, 15483−15489.
12. Vu Hai, M. T., Jolivet, A., Jallal, B., Salesse, R., Bidart, J. M., Houillier, A., Guiochon-Mantel, A., Garnier, J., and Milgrom, E. (1990) Monoclonal antibodies against luteinizing hormone receptor. Immunochemical characterization of the receptor, *Endocrinology 127*, 2090−2098.
13. Towbin, H., Staehelin, T., and Gordon, J. (1979) Electrophoretic transfer of proteins from polyacrylamide gels to nitrocellulose sheets: Procedure and some applications, *Proc. Natl. Acad. Sci. U.S.A. 76*, 4350−4354.
14. Sheer, D. (1990) Sample centrifugation onto membranes for sequencing, *Anal. Biochem. 187*, 76−83.
15. Lui, M., Tempst, P., and Erdjument-Bromage, H. (1996) Methodical analysis of protein−nitrocellulose interactions to design a refined digestion protocol, *Anal. Biochem. 241*, 156−166.
16. Takagaki, Y., Gerber, G. E., Nihei, K., and Khorana, H. G. (1980) Amino acid sequence of the membranous segment of rabbit liver cytochrome b5. Methodology for separation of hydrophobic peptides, *J. Biol. Chem. 255*, 1536−1541.
17. Ball, L. E., Oatis, J. E., Dharmasiri, K., Busman, M., Wang, J., Cowden, L. B., Galijatovic, A., Chen, N., Crouch, R. K., and Knapp, D. R. (1998) Mass spectrometric analysis of integral membrane proteins: Application to complete mapping of bacteriorhodopsins and rhodopsin, *Protein Sci. 7*, 758−764.
18. Soskic, V., Nyakatura, E., Roos, M., Müller-Esterl, W., and Godovac-Zimmermann, J. (1999) Correlations in palmitoylation and multiple phosphorylation of rat bradykinin B_2 receptor in chinese hamster ovary cells, *J. Biol. Chem. 274*, 8539−8545.
19. Karoor, V., and Malbon, C. C. (1996) Insulin-like growth factor receptor-1 stimulates phosphorylation of the β_2-adrenergic receptor in vivo on sites distinct from those phosphorylated in response to insulin, *J. Biol. Chem. 271*, 29347−29352.
20. Jiang, X., Dreano, M., Buckler, D. R., Cheng, S., Ythier, A., Wu, H., Hendrickson, W. A., and El Tayar, N. (1995) Structural predictions for the ligand-binding region of glycoprotein hormone receptors and the nature of hormone-receptor interactions, *Structure 3*, 1341−1353.
21. Kajava, A. V., Vassart, G., and Wodak, S. J. (1995) Modeling of the three-dimensional structure of proteins with the typical leucine-rich repeats, *Structure 3*, 867−877.
22. Bhowmick, N., Huang, J., Puett, D., Isaacs, N. W., and Lapthorn, A. J. (1996) Determination of residues important in hormone binding to the extracellular domain of the luteinizing hormone/chorionic gonadotropin receptor by site-directed mutagenesis and modeling, *Mol. Endocrinol. 10*, 1147−1159.
23. Phang, T., Kundu, G., Hong, S., Ji, I., and Ji, T. H. (1998) The amino-terminal region of the luteinizing hormone/choriogonadotropin receptor contacts both subunits of human choriogonadotropin. II. Photoaffinity labeling, *J. Biol. Chem. 273*, 13841−13847.
24. Hong, S., Phang, T., Ji, I., and Ji, T. H. (1998) The amino-terminal region of the luteinizing hormone/choriogonadotropin receptor contacts both subunits of human choriogonadotropin. I. Mutational analysis, *J. Biol. Chem. 273*, 13835−13840.
25. Davis, D. P., Rozell, T. G., Liu, X., and Segaloff, D. L. (1997) The six N-linked carbohydrates of the lutropin/choriogonadotropin receptor are not absolutely required for correct folding, cell surface expression, hormone binding, or signal transduction, *Mol. Endocrinol. 11*, 550−562.
26. Zhang, R., Cai, H., Fatima, N., Buczko, E., and Dufau, M. L. (1995) Functional glycosylation sites of the rat luteinizing hormone receptor required for ligand binding, *J. Biol. Chem. 270*, 21722−21728.
27. Chen, W., and Bahl, O. P. (1993) High expression of the hormone binding active extracellular domain (1−294) of rat lutropin receptor in *Escherichia coli*, *Mol. Cell. Endocrinol. 91*, 35−41.
28. Ji, I., Slaughter, R. G., and Ji, T. H. (1990) N-linked oligosaccharides are not required for hormone binding of the lutropin receptor in a Leydig tumor cell line and rat granulosa cells, *Endocrinology 127*, 494−506.
29. Tapanainen, J. S., Bo, M., Dunkel, L., Billig, H., Perlas, E. A., Boime, I., and Hsueh, A. J. W. (1993) Deglycosylation of the human luteinizing hormone receptor does not affect ligand binding and signal transduction, *Endocrine J. 1*, 219−225.
30. Keinanen, K. P. (1988) Effect of deglycosylation on the structure and hormone-binding activity of the lutropin receptor, *Biochem. J. 256*, 719−724.
31. Petäjä-Repo, U. E., Merz, W. E., and Rajaniemi, H. J. (1991) Significance of the glycan moiety of the rat ovarian luteinizing hormone/chorionic gonadotropin (CG) receptor and human CG for receptor−hormone interaction, *Endocrinology 128*, 1209−1217.
32. Minegishi, T., Delgado, C., and Dufau, M. L. (1989) Phosphorylation and glycosylation of the luteinizing hormone receptor, *Proc. Natl. Acad. Sci. U.S.A. 86*, 1470−1474.
33. Petäjä-Repo, U. E. (1994) Structural characterization of the carbohydrates of the rat ovarian luteinizing hormone/chorionic gonadotropin receptor, *Biochem. J. 298*, 361−366.

BI992913F